Available online at www.sciencedirect.com

SciVerse ScienceDirect

AASRI Procedia 3 (2012) 652 – 660

AASRI Procedia

www.elsevier.com/locate/procedia

2012 AASRI Conference on Modelling, Identification and Control

Strength Analysis of Enclosure for a High-Speed Permanent Magnet Rotor

Yingeng Zhou[a,]*, Jiancheng Fang[a]

[a]*School of Instrument Science & Opto-electronics Engineering, BeiHang University of Aeronautics & Astronautics, Beijing, 100191, China,*

Abstract

Permanent magnet (PM) machines have become prevalent in very high-speed applications due to its simple structure and high power density. Permanent magnets is the most mechanically vulnerable rotor part, and can not withstand the large centrifugal forces during high-speed rotation. Therefore, the magnet must be contained in a non-magnetic enclosure shrink-fitted onto the PM, which would limit stresses in the magnet and ensure the transfer of torque from the magnet to the shaft at elevated speeds. The strength analysis methods of enclosure for high-speed PM rotor by means of analytical method as well as finite element non-linear contact analysis are introduced. As an example, the strength analysis results for a high speed PM rotor at speed of 60000r/min are presented. The analysis results show that the theoretical calculation value meet the requirements of protecting the permanent magnet in high rotation speed.

Keywords: Permanent magnet machines; high speed; shrink fit; strength analysis; finite element analysis

1. Introduction

High-speed PM machines are a very promising design alternative for high-speed applications because of

* Corresponding author. Tel.: +86-01-82339057; fax: +86-01-82339057.
*E-mail address:*yinfengzhou@163.com.

doi:10.1016/j.aasri.2012.11.104

their better efficiencies, power factors, and utilization factors in comparison to the other types of high-speed electrical machines. But, on the other hand, high-speed PM machines have a much more complex rotor construction in comparison to the other types of high-speed machines. High-speed PM machines have permanent magnets and a retaining enclosure on the rotor. Nowadays, the sintered neodymium-iron-boron (Nd-Fe-B) material is used in most of PM machines. This material exhibits poor mechanical characteristics: a low value of Young's module and brittleness, Therefore, it is necessary to use a nonmagnetic alloy enclosure to protect the PM. Many authors have studied properties of the enclosure and its influence on the magnetic field. Binder et al. [1] showed advantages of using surface-mounted magnets for high speed and also the validity of analytical mechanical modelling for the case of magnets without pole spacers. Larsonneur [2] observed the existence of an optimal interference fit between the magnet and the enclosure for maximum permissible speed. Zwyssig et al. [3] considered not only the enclosure's strength, but also the compatibility of its thermal properties with the permanent magnet.

The most important task of the rotor design is the reliable operation of the high-speed PM rotor. With the increase of rotor speed, the interference fit between the PM and enclosure will decrease. On the other hand, the interference fit between the PM and enclosure could be changed due to the different temperature expansibility of PM and enclosure. The contact pressure between the PM and enclosure must be large enough over the whole speed range in order to guarantee the PM withstanding compressive stress.

This paper aims to determine the fitting and mechanical stress of enclosure as well as permanent magnet in a high speed rotor, while also considering rotational speed and operating temperature. Starting with a presentation of analytical method of mechanical stress and fitting in the rotor based on thick walled theory, in the second step the interference fit between enclosure and PM for a high speed PM rotor at speed of 60000r/min is determined, in the last step a 2D finite element model based on the finite element non-linear contact is introduced to perform the strength analysis for the high speed PM rotor.

2. Theoretical Backgrounds

A high-speed PM rotor will be represented as a compound of three adjacent cylinders which correspond to the shaft, magnet and enclosure. The cross-section of the PM rotor is shown as Fig.1.

The enclosure shrink-fitted onto the PM can be classified as thick-walled cylinder with internal pressures, while the PM can be classified as thick-walled cylinder with external pressures. Considering the variation of speed and temperature, the interference fit between the enclosure and the PM can be determined by the thick-walled cylinder theory.

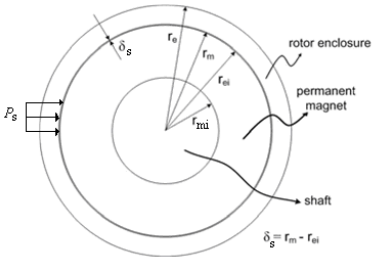

Fig.1 Cross-section of a high-speed PM rotor

2.1The static interference fit and stress

As Fig.1 shown, the static interference fit and shrink pressure between the enclosure and PM is δ_s and

P_s respectively. The inner and outer radius of PM is r_{mi} and r_m, respectively. The inner and outer radius of enclosure is r_{ei} and r_e, respectively. The operating temperature of the rotor is assumed to be uniformly distributed in the rotor and represented as the temperature increment $\Delta T = T - T_0$, where T and T_0 are operating and room temperature respectively. The structure rotates with a constant angular velocity ω.

Here, the material parameters and structure parameters of rotor's enclosure and PM are listed in Table 1. The rated speed n=60000 rpm, operation temperature of rotor T=150℃.

Table 1 Material parameters and structure parameters of rotor's enclosure and PM

	E (Pa)	ρ (kg/m3)	ν	[σ] (MPa)	inner radius (mm)	outer radius (mm)
enclosure	1.86e11	8200	0.31	1100	18	22.5
PM	1.0e11	7400	0.30	80	22.5	25

Based on the thick-walled cylinder theory[4], the stress and strain for the PM subjected to external pressures P_s, while the stress and strain for the enclosure subjected to internal pressures P_s are given by

$$\begin{aligned}
&\sigma_{rm}^s(r) = -\frac{r_m^{\,2} p_s}{r_m^{\,2} - r_{mi}^{\,2}}\left(1 - \frac{r_{mi}^{\,2}}{r^2}\right) \qquad \sigma_{\theta m}^s(r) = -\frac{r_m^{\,2} p_s}{r_m^{\,2} - r_{mi}^{\,2}}\left(1 + \frac{r_{mi}^{\,2}}{r^2}\right) \qquad r_{mi} \le r \le r_m \\
&u_m^s(r) = \frac{r_{mi}^{\,2} p_s}{E_m(r_m^{\,2} - r_{mi}^{\,2})}\left[\frac{(1+\nu_m) r_m^{\,2}}{r} + (1-\nu_m) r\right] \\
&\sigma_{re}^s(r) = \frac{r_e^{\,2} p_s}{r_e^{\,2} - r_{ei}^{\,2}}\left(1 - \frac{r_{ei}^{\,2}}{r^2}\right) \qquad \sigma_{\theta e}^s(r) = \frac{r_e^{\,2} p_s}{r_e^{\,2} - r_{ei}^{\,2}}\left(1 + \frac{r_{ei}^{\,2}}{r^2}\right) \qquad r_{ei} \le r \le r_e \\
&u_e^s(r) = \frac{r_{ei}^{\,2} p_s}{E_e(r_e^{\,2} - r_{ei}^{\,2})}\left[\frac{(1+\nu_e) r_e^{\,2}}{r} + (1-\nu_e) r\right]
\end{aligned} \tag{1}$$

Where $\sigma_{\theta e}^s$、σ_{re}^s and $\sigma_{\theta m}^s$、σ_{rm}^s are static tangential stress and radial stress of enclosure and PM, respectively. u_e^s and u_m^s are radial displacements of enclosure and PM, respectively. E_e and E_m are Young's modulus of enclosure and PM, respectively. ν_e and ν_m are Poisson's ratio of enclosure and PM, respectively.

Then the static interference fit δ_s can be given as

$$\delta_s = u_e^s(r_{ei}) - u_m^s(r_m) \tag{2}$$

From equations (1) and (2), the static shrink pressure p_s can be determined as

$$p_s = \frac{\delta_s}{\dfrac{r_{ei}}{E_e}\left(\dfrac{r_e^{\,2} + r_{ei}^{\,2}}{r_e^{\,2} - r_{ei}^{\,2}} + \nu_e\right) + \dfrac{r_m}{E_m}\left(\dfrac{r_m^{\,2} + r_{mi}^{\,2}}{r_m^{\,2} - r_{mi}^{\,2}} - \nu_m\right)} \tag{3}$$

2.1. The interference fit and stress under the action of centrifugal force

Considering the action of centrifugal force, the stress and strain of the PM and enclosure can be expressed respectively as [5]

$$
\begin{aligned}
&\sigma_{rm}^{r}(r)=\frac{3-2\nu_m}{8(1-\nu_m)}\rho_m\omega^2\left(r_m{}^2+r_{mi}{}^2-\frac{r_{mi}{}^2r_m{}^2}{r^2}-r^2\right)\\
&\sigma_{\theta m}^{r}(r)=\frac{3-2\nu_m}{8(1-\nu_m)}\rho_m\omega^2\left(r_m{}^2+r_{mi}{}^2+\frac{r_{mi}{}^2r_m{}^2}{r^2}-\frac{1+2\nu_m}{3-2\nu_m}r^2\right) \qquad r_{mi}\le r\le r_m\\
&u_m{}^r(r)=\frac{(3-2\nu_m)(1+\nu_m)}{8E_m(1-\nu_m)}\rho_m\omega^2 r\left[(1-2\nu_m)(r_{mi}{}^2+r_m{}^2)+\frac{r_{mi}{}^2r_m{}^2}{r^2}-\frac{1-2\nu_m}{3-2\nu_m}r^2\right]\\
&\sigma_{re}^{r}(r)=\frac{3-2\nu_e}{8(1-\nu_e)}\rho_e\omega^2\left(r_e{}^2+r_{ei}{}^2-\frac{r_{ei}{}^2r_e{}^2}{r^2}-r^2\right)\\
&\sigma_{\theta e}^{r}(r)=\frac{3-2\nu_e}{8(1-\nu_e)}\rho_e\omega^2\left(r_e{}^2+r_{ei}{}^2+\frac{r_{ei}{}^2r_e{}^2}{r^2}-\frac{1+2\nu_e}{3-2\nu_e}r^2\right) \qquad r_{ei}\le r\le r_e\\
&u_e^{r}(r)=\frac{(3-2\nu_e)(1+\nu_e)}{8E_e(1-\nu_e)}\rho_e\omega^2 r\left[(1-2\nu_e)(r_{ei}{}^2+r_e{}^2)+\frac{r_{ei}{}^2r_e{}^2}{r^2}-\frac{1-2\nu_e}{3-2\nu_e}r^2\right]
\end{aligned}
\tag{4}
$$

The dynamic interference fit between the PM and enclosure owing to rotating deformation will be

$$\delta_d=u_e{}^r(r_{ei})-u_m{}^r(r_m) \tag{5}$$

2.2. The interference fit and stress consideration temperature

Under the sistuation of the temperature increase, the magnitude of the integral sintered NdFeB expansion in the direction of parallel magnetizing is equal to shrinkage in the direction of vertical magnetizing, so the displacement of the PM due to the influence of temperature increase can be ignored.

Considering the influence of temperature, the displacement of the enclosure is determined as follows

$$u_e{}^t(r)=r\alpha_e\Delta T \qquad r_{ei}\le r\le r_e \tag{6}$$

Considering both the rotating and temperature conditions, the total interference fit between the PM and enclosure will be

$$\Delta\delta=\delta_s-\delta_d-u_e{}^t(r_{ei})=(r_{ei}-r_m)-\left(u_e{}^r(r_{ei})-u_m{}^r(r_m)\right)-u_e{}^t(r_{ei}) \tag{7}$$

Considering the influence of temperature increase, the stress in the enclosure is presented as [6]

$$\begin{bmatrix}\sigma_{re}^t\\ \sigma_{\theta e}^t\end{bmatrix}=\begin{bmatrix}1/E_e & -\nu_e/E_e\\ -\nu_e/E_e & 1/E_e\end{bmatrix}^{-1}-\begin{bmatrix}1/E_e & -\nu_e/E_e\\ -\nu_e/E_e & 1/E_e\end{bmatrix}^{-1}\begin{bmatrix}\alpha_{re}\\ \alpha_{\theta e}\end{bmatrix}\Delta T \tag{8}$$

Thus, the analytical expressions for radial and tangential stress in the PM rotor under operating mode are obtained. Influences of static pressure (fitting), centrifugal force (rotation) and temperature increase on the stress can be clearly distinguished in the expressions which can be expressed in the following way:

$$\begin{aligned}\sigma_{re}(r)&=\sigma_{re}^{s}(r)+\sigma_{re}^{r}(r)+\sigma_{re}^{t}\\ \sigma_{\theta e}(r)&=\sigma_{\theta e}^{s}(r)+\sigma_{\theta e}^{r}(r)+\sigma_{\theta e}^{t}\end{aligned}\quad r_{ei}\le r\le r_e \qquad \begin{aligned}\sigma_{rm}(r)&=\sigma_{rm}^{s}(r)+\sigma_{rm}^{r}(r)\\ \sigma_{\theta m}(r)&=\sigma_{\theta m}^{s}(r)+\sigma_{\theta m}^{r}(r)\end{aligned}\quad r_{mi}\le r\le r_m \tag{9}$$

The total equivalent Von Mises stress in the enclosure is

$$\sigma_e=\sqrt{1/2\left[\left(\sigma_{re}-\sigma_{\theta e}\right)^2+\left(\sigma_{re}\right)^2+\left(\sigma_{\theta e}\right)^2\right]} \tag{10}$$

2.3. Determination of the interference fit between enclosure and PM

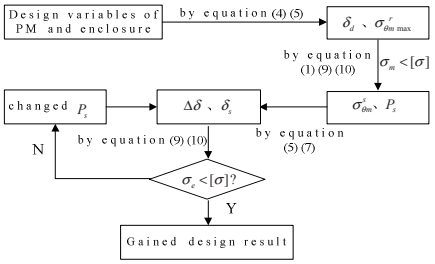

Fig.2 Flow chart for theoretical calculation of interference fit

The interference fit between the PM and enclosure has important effect on the reliable operation of the PM rotor. If the interference fit is very low, the enclosure will be loose and the PM will be destroyed because of the enormous tensile strength during the increase of speed and temperature. If the interference fit is very high, then the electromagnetism performance of the high-speed PM machine will be subjected to impact. Fig.2 gives the theoretical calculation process of interference fit.

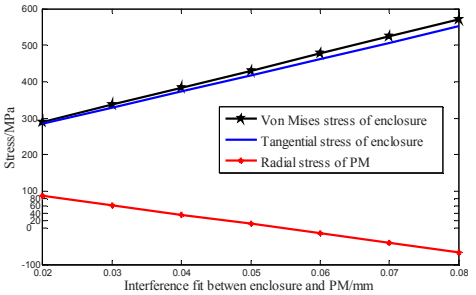

Fig.3 The interference fit versus stress between enclosure and PM considering temperature and speed

Fig. 3 shows the interference fit versus stress between enclosure and PM considering temperature and speed. The Von stress in enclosure increase with the increase of the interference fit, while the tangential stress in PM decrease. When the interference fit is more than 0.08mm, the Von stress in enclosure exceeds the permissible tensile strength. When the interference fit is less than 0.02mm, the radial stress in PM exceed the permissible tensile strength. While the interference fit is 0.05mm, the stresses in enclosure and PM are all meet demand and more reasonable.

3. Finite-Element Model

Finite element modelling was performed using ANSYS structural analysis, the FE model is shown as Fig. 4.The model used PLANE183 elements for 2D structural modelling while the contact area between the magnet and enclosure was modelled using CONTA172 and TARGE169.

Fig. 4 Gemotry and FE model of the PM rotor (axial symmetry)

3.1. Stress of PM rotor with room temperature, zero speed

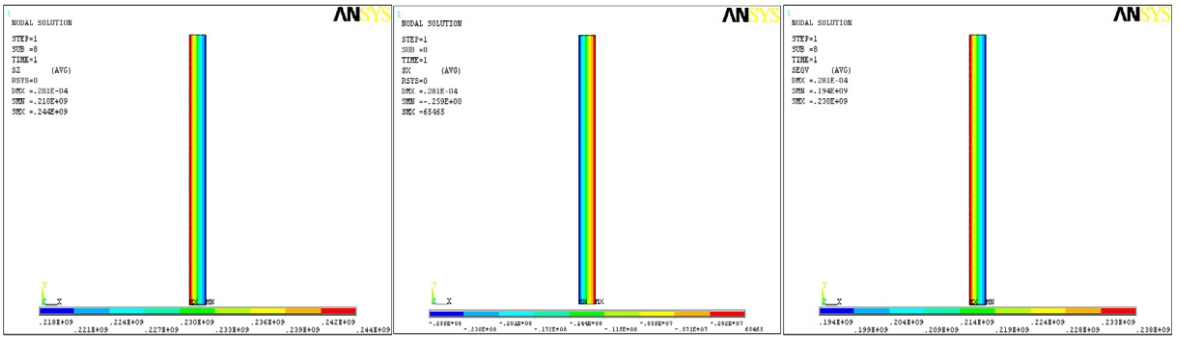

(a) Tangential stress in enclosure; (b) Radial stress in enclosure; (c) Von Mises stress in enclosure

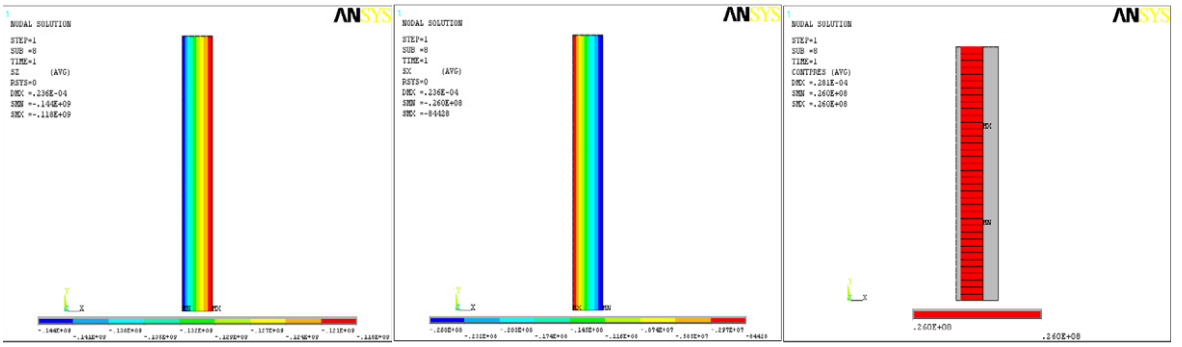

(d) Tangential stress in PM; (e) Radial stress in PM; (f) Contact pressure

Fig. 5 static stress and contact pressure in PM and enclosure

Fig. 5 shows the static stress and contact pressure in PM and enclosure. The tangential stress in enclosure is 218～244 MPa, radial stress is -25.9～0.065 MPa, Von Mises stress is 194～238 MPa which is below half the permissible tensile strength 500MPa. The tangential stress in PM is -144～-118 MPa, radial stress is -26～-0.084 MPa, Von Mises stress is 106～145 MPa, which is much less than the compressive strength limit 800MPa. The contact pressure between the enclosure and PM is 26MPa. Maximum equivalent stress in the enclosure is at the inner surface and the equivalent stress decrease with the increase of enclosure's thickness.

3.2. Stress of PM rotor with room temperature, 60000rpm speed

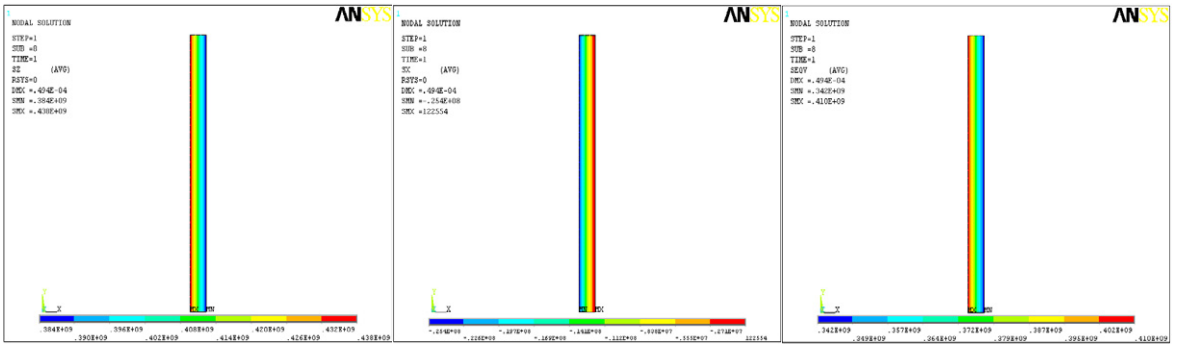

(a) Rotating tangential stress in enclosure; (b) Rotating radial stress in enclosure; (c) Rotating Von Mises stress in enclosure

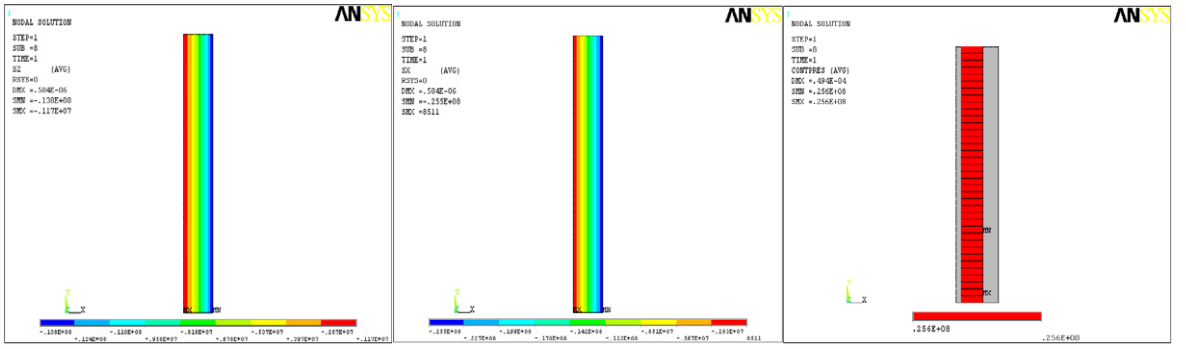

(d) Rotating tangential stress in PM; (e) Rotating radial stress in PM; (f) Contact pressure at 60000rpm speed

Fig. 6 The rotating stress and contact pressure in PM and enclosure

Fig. 6 shows the rotating stress and contact pressure in PM and enclosure. When the rotor rotate at the speed of 60000rpm, the rotating tangential stress in enclosure is 384～438 MPa, rotating radial stress is -25.4～0.12 MPa, rotating Von Mises stress is 342～410 MPa which is still below half the permitted tensile strength 555MPa. The rotating tangential stress in PM is -13.8～-1.17MPa, rotating radial stress is -25.5～0.009MPa, rotating Von Mises stress is 5.8～21.8 MPa, which is less than the compressive stress. The contact pressure between the enclosure and PM decrease to 25.6MPa. Under the action of centrifugal force, both the PM and the enclosure produce strain, the interference fit and stress at the contact surface decrease, thus the PM endure tensile stress partially, and the rotating Von Mises stress in enclosure increase.

3.3. Stress of PM rotor with 150℃ temperature and 60000rpm speed

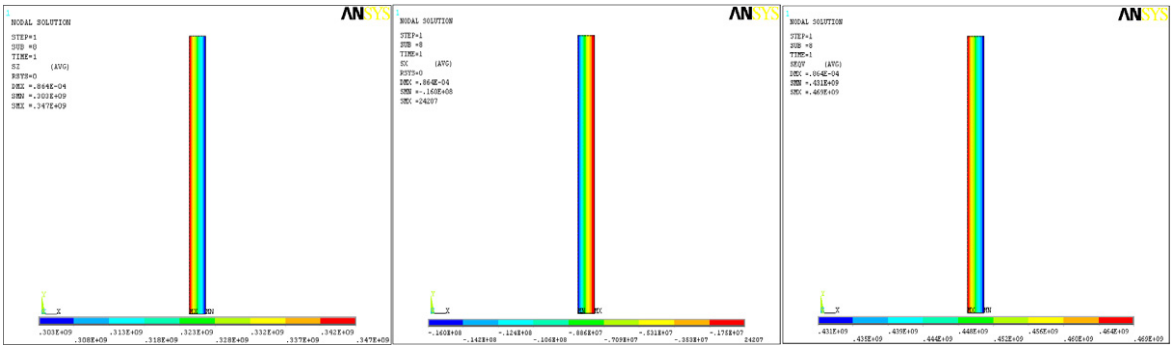

(a) Tangential stress in enclosure ; (b) Radial stress in enclosure; (c) Von Mises stress in enclosure;

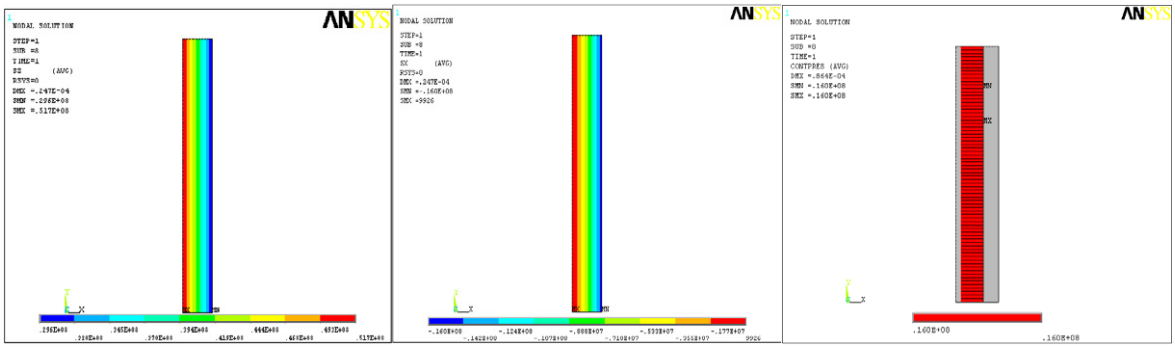

(d) Tangential stress in PM; (e) Radial stress in PM; (f) Contact pressure

Fig. 7 stress and contact pressure in PM and enclosure with 150℃temperature and 60000rpm speed

When temperature heated up, due to the effect of thermal expansion and contraction, the interference fit between the enclosure and PM further decrease, the compressive stress in PM further decrease certainly. Figure 7 shows the stress and contact pressure in PM and enclosure with 150℃temperature and 60000rpm speed ,the tangential stress in enclosure is 303～347 MPa, radial stress is-16～0.024 MPa, Von Mises stress decrease to 431～469 MPa which is still below the permitted tensile stress. The tangential stress in PM is 29.6～51.7MPa, radial stress is -16～0.01MPa. The contact pressure between the enclosure and PM decrease to 16MPa.

3.4. Results comparison

Results are given in Table 2 including three models that represent still rotor and the rotor rotating at the target speed of 60000 rpm at both room and maximum temperature. It can be seen that the FEM result is generally in good agreement with analytical result.

The radial compressive stress in the PM decrease with the increase of rotating speed and temperature, but the contact pressure between magnet and enclosure is maintained throughout the whole speed range. To the

enclosure, the state of rotating at 60000rpm and under room temperature is the critical stage, while to the PM, the state of rotating with maximum speed and with maximum temperature is the critical stage. Both the PM and the enclosure satisfy an intensity request at their critical stage.

Table 2 Comparison of the stress of PM rotor between FEM method and analytical method

Mechanical stress MPa		enclosure		magnet		contact pressure
		tangential	radial	tangential	radial	
30℃, 0rpm	FEM	218～244	-25.9～0.065	-144～-118	-26～-0.084	26
	analytical	220.49～246.35	-25.86～0	-143.67～-117.81	-25.86～0	25.86
30℃, 60000rpm	FEM	384～438	-25.4～0.12	-13.8～-1.17	-25.6～0.009	25.6
	analytical	389～442.99	-25.86～0	-15.65～-3.52	-25.86～0	25.52
150℃, 60000 rpm	FEM	303～347	-16～0.024	29.6～51.7	-16～0.01	16
	analytical	296.3～350.28	-19.721～0	29.581～49.101	-19.721～0	9.67

4. Conclusion

The stress analysis of the PM rotor is extremely important to the reliable operation of high speed machines. This paper describes the interference fit and mechanical stress of enclosure as well as permanent magnet in a high speed rotor. Based on thick walled theory, analytical method of mechanical stress and fitting in the rotor is presented. A 2D finite element model based on the finite element non-linear contact is successively introduced to perform the strength analysis for a high speed PM machine with rated speed of 60000r/min. The FEM result is generally in good agreement with analytical result. Three models that represent still rotor and the rotor rotating at the target speed of 60000 rpm at both room and maximum temperature are analyzed, both the PM and the enclosure satisfy an intensity request at their critical stage.

Acknowledgements

The research is supported by the National Great Science and Technology Fruit Converts Item.

References

[1] Binder A, Schneide T, Klohr MR. Fixation of buried and surface-mounted magnets in high-speed permanent magnet synchronous machines. IEEE Trans. on Ind. Applications 2006; 42: 1031-1037.
[2] Larsonneur R. Design and control of active magnetic bearing systems for high speed rotation, PhD thesis, ETH Zurich, 1990.
[3] Zwyssig C, Kolar JW, Thaler W, Vohrer M. Design of a 100 W, 500000 rpm permanent-magnet generator for mesoscale gas turbines. Record of the 2005 IAS Annual Meeting 2005; 1: 253-260.
[4] Ugural AC, Fenster FK. Advanced Strength and Applied Elasticity. New Jersey: Prentice Hall, Englewood Cliffs; 1995.
[5] B. Riemer, M. Lebman, Hameyer K. Rotor design of a high-speed permanent magnet synchronous machine rating 100,000 rpm at 10 kW. Energy Conversion Congress and Exposition(ECEE), 2010 IEEE, 3978～3985.
[6]N. Noda, R.B. Hetnarski, Y. Tanigawa. Thermal Stresses. Taylor and Francis; 2003.